

SHAPE IDENTIFICATION USING DISTRIBUTED STRAIN DATA FROM EMBEDDED OPTICAL FIBER SENSORS

Mayuko Nishio*, Tadahito Mizutani*, Nobuo Takeda*
*The University of Tokyo

Keywords: *shape identification, optical fiber sensors, distributed strain data, inverse analysis, measurement error distributions, robust estimation method*

Abstract

The accurate shape sensing method is expected to be useful for large scaled structural health monitoring of aircraft structures. This research is trying to construct a high-accuracy structural shape identification method using distributed strain data from an optical fiber strain sensing system; pulse-prepump Brillouin optical time domain analysis (PPP-BOTDA) system. In addition, the optical fiber can be embedded in composite material, which has recently been applied for the structural material of aircrafts or some other large-scaled structures. In this paper, we firstly considered the characteristics of distributed data from PPP-BOTDA system by the beam bending test using composite specimen with an embedded optical fiber. In addition, the verification of measurement error distributions was carried out. And then, we proposed an appropriate shape identification algorithm for beam bending deflection. The robust estimation method was adopted to correspond to outliers, and showed the effectiveness of the method.

1 Introduction

This paper reports considerations for the construction of a shape identification system using embedded optical fiber sensors in CFRP composite structures. We use distributed strain data obtained by one of the optical fiber strain sensing systems; pulse-prepump Brillouin optical time domain analysis (PPP-BOTDA).

CFRP composite material is increasingly used as the structural material of aircraft structures. They require high safety and reliability in operation, even though they are used under severe environmental conditions. This is the reason why the structural health monitoring (SHM) technology is regarded as important in the aerospace field. Thus, the strain or

temperature measurement technologies using optical fiber sensors have been paid attention for SHM system. Moreover, the optical fiber is possible to be embedded in composite material. This makes it possible to realize a “smart structure” that is an integral structure of sensors.

The accurate shape identification method is expected to be useful for large scaled structural monitoring of future aerospace structures. So far, several researches, which try to detect fatal damage of composite material, have been conducted. However, as CFRP composite is increasingly used, large scaled composite structures, such as wing structures of aircrafts, are positively considered. Therefore, the full-scaled shape identification system will also be of advantage for SHM of large scaled composite structures. It can make it possible to detect undesirable deformations of wings or body of aircrafts in real-time. Moreover, this system is useful for detection of the thermal displacement in manufacturing process of large composite structures.

One of the points of our research is using distributed strain data. We use distributed strain measurement system; PPP-BOTDA system. Using this system, strain distribution along an optical fiber can be obtained. There are few challenges for using distributed strain data to make shape identification algorithm. Some prior researches tried the shape identification problem using discrete strain data obtained by FBG sensors or strain gages [1] [2]. However, in the use of these sensors, the number and the placement of sensors greatly affect the accuracy of the estimated value. Moreover, it is difficult to put sensors on pre-determined positions with accuracy. On the other hand, we can use optical fibers without any spatial processing like FBG sensors in the PPP-BOTDA system. The sensor part is the whole length of the fiber. This makes it possible to lay optical fiber sensors networks on the whole of structures easily. Therefore, such

distributed strain sensor is suitable for full-field structural shape monitoring. The other point of this research is that we did verification using an embedded optical fiber in the composite specimen. This makes it possible to show the possibility of smart structures, in which sensors for SHM are already internally installed.

Reconstruction of displacement from strain data is to say an inverse problem. In general, such an inverse problem has ill-posedness, which means that the problem does not necessarily satisfy the condition of existence, uniqueness, and stability of its solution. This point means that the estimated values greatly depend on the measurement data characteristics.

In this paper, firstly we explain the PPP-BOTDA system; the measurement mechanism and the spatial resolution of distributed data. Then, we report the result of beam bending test using a composite specimen with an embedded optical fiber. From this experiment, it was also judged whether the appropriate strain distribution can be obtained by the PPP-BOTDA system. In addition, we verified measurement error distributions of PPP-BOTDA system by iterative measurements of an unloaded optical fiber. From results of these experiments, we considered the characteristics of distributed strain data obtained by PPP-BOTDA system and the appropriate shape identification method. After that, we proposed a deformation identification method, and the estimation was carried out using the distributed strain data from PPP-BOTDA system. And then, the values of estimated deflection were examined, and effectiveness of the identification method was verified.

2 Principle of PPP-BOTDA System

The pulse-prepump Brillouin optical time domain analysis (PPP-BOTDA) sensing system implements the stimulated Brillouin scattering technique [3]. Figure 1 shows the principle of this system. Two laser beams, a pump pulse and a probe light (continuous wave), are injected into an optical fiber from both its ends. The interaction of these two laser beams excites Brillouin scattering. The Brillouin scattering is excited in each frequency of the probe light. The value of the strain can be estimated by measuring the peak frequency of Brillouin gain spectrum, while its position along the fiber is calculated from the light round-trip time. Figure 2 is a picture of the equipment of PPP-BOTDA sensing system; NBX-6000. This

measuring system can set the spatial resolution, the sampling interval along the fiber. In its maximum performance, the system ensures up to 100 mm spatial resolution, 50 mm sampling interval, and $\pm 0.0025\%$ strain measurement accuracy [4].

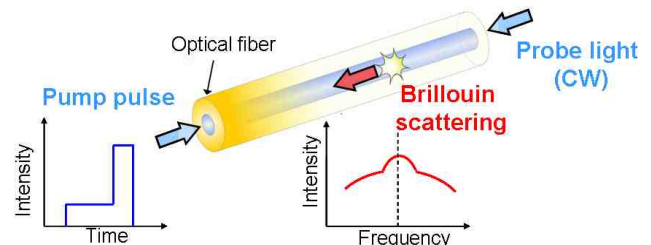


Fig. 1. Principle of PPP-BOTDA system

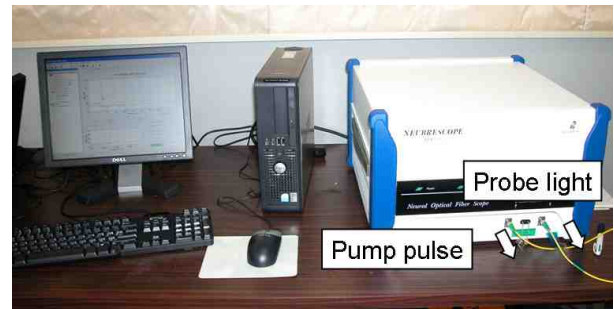


Fig. 2. Equipment of PPP-BOTDA system

3 Distributed Strain Measurement using PPP-BOTDA System

3.1 Beam Bending Test using Embedded Optical Fiber

3.1.1 Fabrication of the Specimen

In order to make a sufficient number of sampling points of PPP-BOTDA system, the length of the specimen had to be long enough against its spatial resolution or sampling interval. To fabricate a composite beam of almost 1 m in length, Vacuum assisted Resin Transfer Molding (VaRTM) method was adopted as the fabrication method. This method is attracting much interest as a fabrication method of large-scaled composite structures in recent years. Figure 3 is a diagram of VaRTM method. The process of VaRTM is firstly laminating of carbon fiber sheets on the forming mold. Secondly, the laminated carbon fiber sheets are packed by plastic film and the inside of baggage is vacuumed up. And then, liquid epoxy resin is transferred into the

SHAPE IDENTIFICATION USING DISTRIBUTED STRAIN FROM EMBEDDED OPTICAL FIBER SENSORS

baggage, and the epoxy is interpenetrated and cured. Figure 4 is the picture of laminated carbon fiber sheets. Some optical fibers were placed between the sheets. We fabricated a flat plate with 1000 mm in length and 250 mm in width, and cut out several beam specimens.

The actual size of the specimen was 1000 mm in length, 70 mm in width, and 7 mm in thickness. The laminate configuration was $[0]_{32}$, and fiber direction was parallel to the length direction. The carbon fiber was Toray / Soficar, T800S (tensile modulus: 294 GPa), and the epoxy resin was DENATOOL® XNR6809 (tensile modulus: 2.3 GPa). The tensile modulus of fabricated composite was 144 GPa in the fiber direction. This value was derived by tensile test using test pieces, which were cut out from the fabricated composite plate. Embedded positions of the optical fiber are shown in Fig.5. There were two optical fiber lines, one was placed between 1st layer and 2nd layer, and the other was placed between 31st layer and 32nd layer. The nominal thickness of one layer was about 0.2 mm, and, therefore, the optical fiber was embedded 0.2 mm inner from the surface. Figure 6 is a picture of the cross section of the embedded area. We used the polyimide-coated single-mode optical fiber, and its diameter was approximately 150 μm .

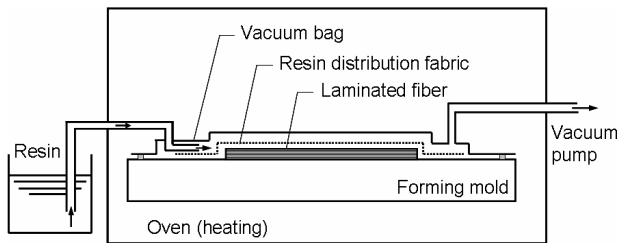


Fig. 3. VaRTM method

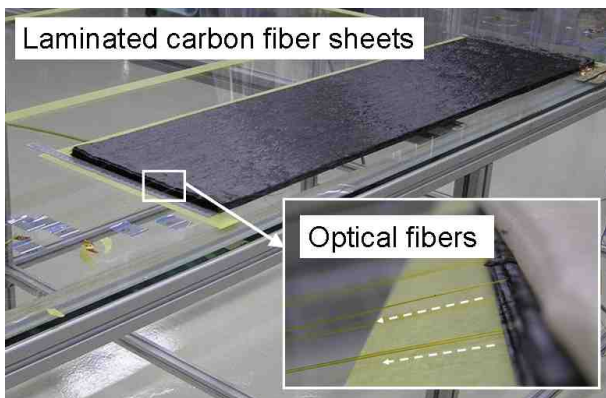


Fig. 4. Pictures of specimen fabrication

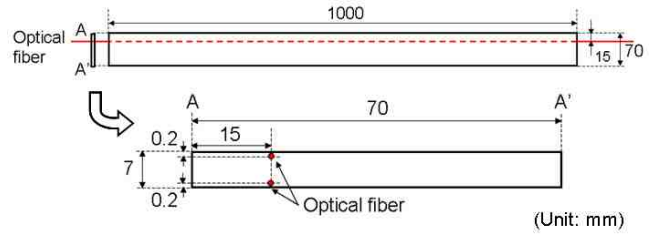


Fig. 5. Embedded positions of the optical fiber

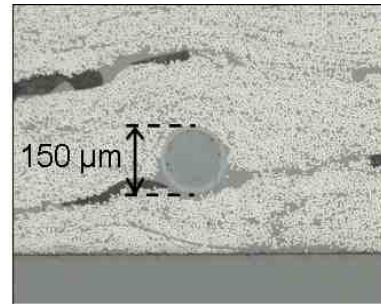


Fig. 6. Embedded optical fiber

3.1.2 Configuration of the Experiment

Figure 7 shows the configuration of cantilever beam bending test. The strain sensors were not only the optical fiber sensor, but also eight strain gages, which were attached in 100 mm interval. The deflection was also measured using a dial gage and two scales. One end portion was clamped to provide the fixed-end boundary condition. Therefore, the actual length of the beam was 850 mm. The load direction is y direction in Fig.8, and the applied load was 49 N and 100 N. Figure 8 is a picture of the experimental setup.

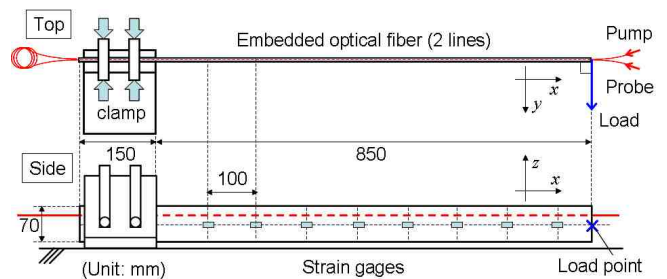


Fig. 7. Configuration of beam bending test

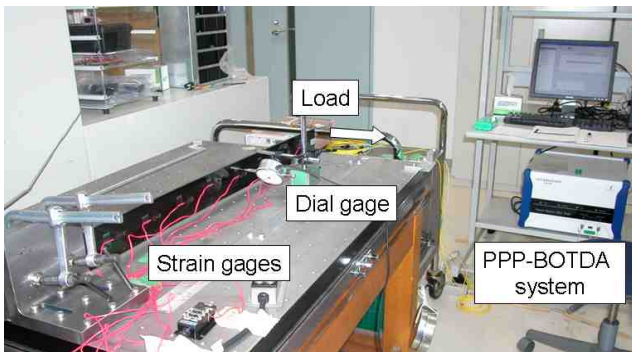


Fig. 8. Setup of measuring system

3.1.3 Results

The output of the PPP-BOTDA system is the peak frequency of the Brillouin scattering spectrum along the optical fiber. The peak frequency shift is shown in Fig.9 (load: 100 N). The spatial resolution was 100 mm, sampling interval was 50 mm. It can be shown that the peak frequency shifts within the region of the embedded optical fiber in the specimen. The spectrum change of the stimulated Brillouin scattering (SBS) at the measuring point A in Fig.9 is shown in Fig.10. The value of peak frequency gets lower in loaded condition. The left side in Fig.9 is compression area and the right side is tension area. From the amount of this peak frequency shift, the strain distribution can be calculated. Figure 11 is distribution plots of strain data from PPP-BOTDA system, strain gages, and theoretical distribution calculated by Euler beam theory. From this figure, the distribution profile of PPP-BOTDA system is almost linear, which is typical strain distribution of a cantilever beam bending with a concentrated load. The value of strain also corresponds to values from strain gages and theoretical distribution. From this result, it can be said that we can obtain appropriate strain distributions by the PPP-BOTDA system.

On the other hand, the distribution profile is different from theoretical distribution at both ends of the beam. At the distance of 0 mm, the absolute value of PPP-BOTDA system is lower than the theoretical value, and the distribution profile is non-linear at the both ends. This is because the distributed strain data is the mean strain of its spatial resolution. At the sampling points near the ends of beam, where the strain distribution is discontinuous along the fiber, the strain value includes information of unloaded area, as shown in the diagram in Fig.12. Such changes of the distribution profile at discontinuous points are the feature of distributed strain data. The difference with theoretical value at

distance of 0 m becomes almost 200 $\mu\epsilon$. Such differences are considered to be significant outliers in the inverse analysis.

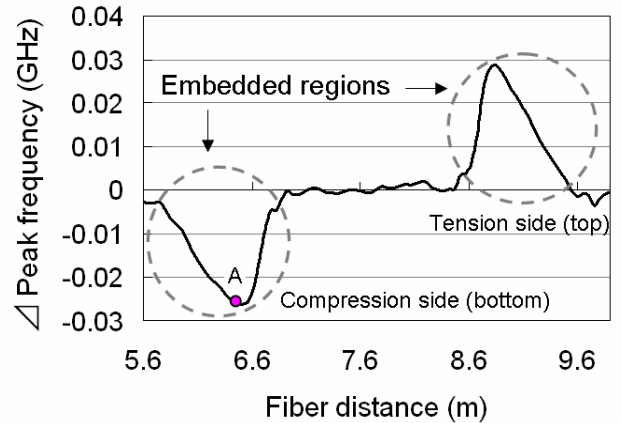


Fig. 9. Peak frequency shift

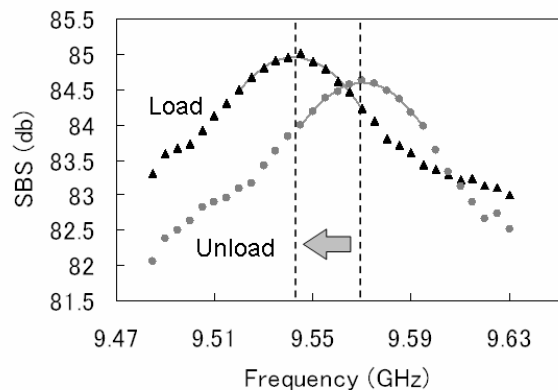


Fig. 10. Brillouin scattering spectrum at point A

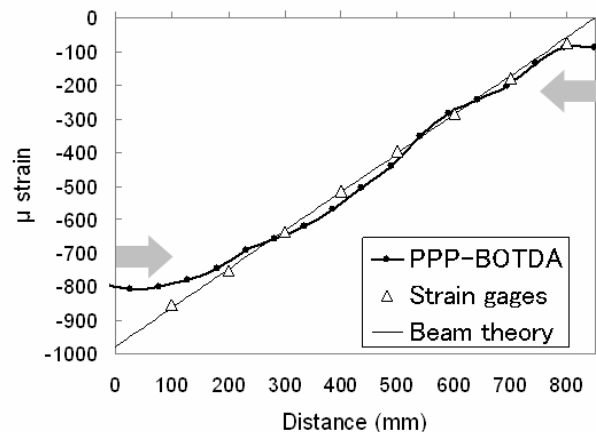


Fig. 11. Strain distributions

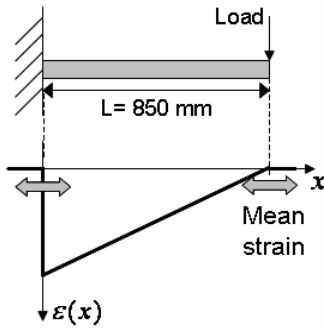


Fig. 12. Mean strain at discontinuous points

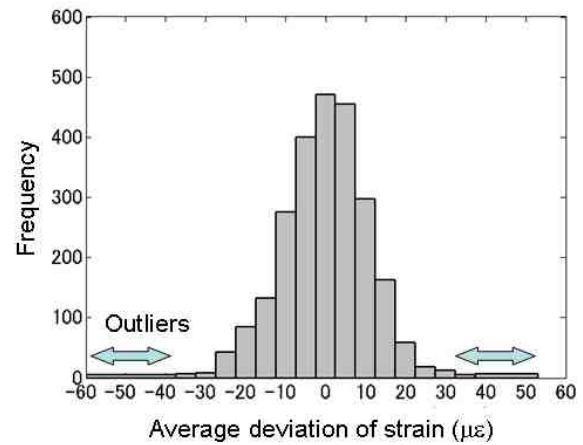
3.2 Measurement Error Distribution

In the inverse analysis, the measurement error distribution and the stability of data are great significant. This is because the least-square method, which is often used in inverse analysis, can be used strictly only when the error distribution of data shows normal distribution. To obtain the measurement error distribution of the PPP-BOTDA system, iterative measurements of an unloaded optical fiber (strain free) was carried out. One set of measurements was held in almost same conditions (fiber, temperature, humidity). And then, a histogram was made by deviations from the mean value of data. From the histogram, we derived the mean value, the standard deviation, the skewness, and the kurtosis to verify the degree of normal distribution. Figure 13 shows error distributions of two sets of measurements, and their statistic values are shown in Table 1. The parameter of two data is the number of averaging in PPP-BOTDA system. The accuracy of data becomes higher when the number of averaging is increased. It can be shown by the value of standard deviations in Table 1. The degree of normal distribution can be verified by the values of skewness and kurtosis. When these values shows zero, the distribution is the normal distribution. However, the values of kurtosis are higher than zero in both distributions, and the values of skewness have also differences. Therefore, it can be said that the degree of normal distribution of these error distribution is low. Moreover, the profiles of error distributions in Fig.13 show many outliers, and the ranges of deviations become wide. The histograms are more similar to Cauchy distribution than normal distribution.

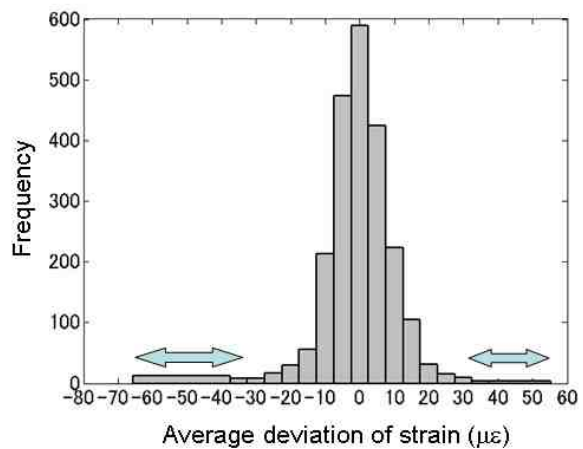
In addition, we observed that some data showed unpredictable shifts of distributions; the distribution shifted even in same measurement condition. Figure 14 shows one of such data. The profile of peak frequency distribution shifts in the

direction of the optical fiber. Such distribution shifts are considered to be derived from the instability of light scattering and slight changes of measurement conditions.

Form these verifications, the PPP-BOTDA data showed outliers in some measurements points and some unusual distributions. It is considered that the strain measurement of PPP-BOTDA system is very sensitive against changes of slight measurement conditions. And then, the degree of the normal distribution is low, so it can be said that it is difficult to use the least-square method strictly in the shape identification algorithm. We have to consider a robust method against such outliers.



a) Averaging: 2^{15}



b) Averaging: 2^{16}

Fig. 13. Measurement error distribution of PPP-BOTDA system

Table 1. Level of normal distribution

	Mean	Standard deviation	Skewness	Kurtosis
2 [^] 15	1E-10 $\mu\epsilon$	10.9 $\mu\epsilon$	-0.1	1.4
2 [^] 16	3E-16 $\mu\epsilon$	9.7 $\mu\epsilon$	-0.7	6.1

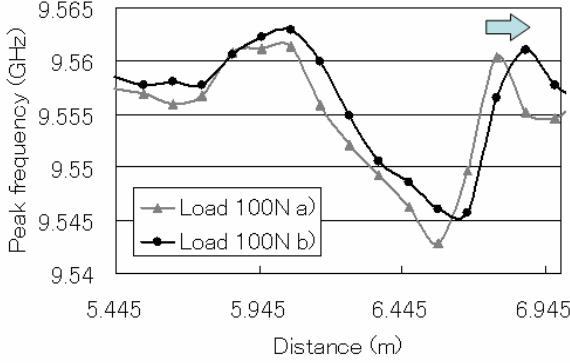


Fig. 14. Unpredictable shift of the peak frequency distribution

4 Displacement Derivation using Distributed Strain Data

Using the distributed strain data obtained from PPP-BOTDA system, we carried out the inverse analysis to estimate the deflection of cantilever beam bending. Consideration of results in section 3, we propose a robust estimation method against outliers of data, and verify the advantage of the method.

4.1 Robust Estimation Method

The estimated strain distribution $\epsilon_e(x)$ of a cantilever beam bending with concentrated load is represented as a linear expression (1). This function can be easily integrated, and the deflection $w_e(x)$ is derived as (2). The value x is the coordinate of beam length direction ($0 \leq x \leq L$, $L=850$ mm), and the subscript e means estimated values. The value $z=6.6$ mm is the length in thickness direction between top and bottom embedded optical fibers. Using equation (1) and (2), when the value a_1 and a_2 are estimated, the deflection $w_e(x)$ can be derived easily in this problem.

$$\epsilon_e(x) = a_{e1} + a_{e2}x \quad (1)$$

$$w_e(x) = -\frac{2}{z} \int \int_0^L \epsilon_e(x) dx dx \quad (2)$$

The estimation of the value a_1 and a_2 is the polynomial fitting problem using measured strain data. To make the estimation method robust against outliers, we used M-estimation method [5]. This method is basically the iterative weighted least-square method. The robustness is derived from adjustment of weight using Biweight method, which makes it possible to add light weight to outliers.

First, the data from PPP-BOTDA system was configured to \mathbf{D} matrix.

$$\mathbf{D} = \begin{bmatrix} x_1^m & \cdots & x_n^m \\ \epsilon_1^m & \cdots & \epsilon_n^m \end{bmatrix}^T$$

The calculation flow of the robust estimation method is as follows. The estimate values are a_1 and a_2 in equation (1).

- 1) Estimate the initial value using the usual least-square method. The value j is the iteration number.

$$\epsilon_{j=0}(x) = a_{1(j=0)} + a_{2(j=0)}x \quad (3)$$

- 2) Calculate the residual value between strain data and estimated strain at measurement points x_i^m ($i=1 \sim n$).

$$v_{i0} = \left| \epsilon_i^m - \epsilon_j(x_i^m) \right| \quad (4)$$

- 3) Decide weights of each measurement points using the Biweight method.

$$\omega_{ij}^{adj} = \begin{cases} \left(1 - (v_{ij}/cs_j)^2\right) & v_{ij} < cs_j \\ 0 & otherwise \end{cases} \quad (5)$$

The value s_j is the median of v_{ij} . The value c is the constant number, which decides threshold amount to make weight zero. From the value ω_{ij}^{adj} , the weight ω_{ij}^{eff} can be derived as follows.

$$\omega_{ij}^{eff} = \frac{n\omega_{ij}^{adj}}{\sum_{i=1}^n \omega_{ij}^{adj}} \quad (6)$$

- 4) Estimate the value a_1 and a_2 by the weighted least-square method using the weight value ω_{ij}^{eff} .

In the least-square method, an error function to be minimized can be defined as follows.

$$E[\varepsilon_e(x)] = \sum_{i=0}^n [\omega_{ij}^{eff} (\varepsilon_e(x_i) - \varepsilon_i^m)] \quad (7)$$

Equation (7) is the sum of differences between estimated strain values and measured strain values. This error function has a minimum if $\partial E / \partial a_k = 0$ for $k = 1, 2$. In addition, the prior information can be used to improve the accuracy of estimated values. In this cantilever beam bending problem, the strain value at free end (distance $x=850$ mm) becomes zero ($\varepsilon(850) = 0$). Using this information as a constraint condition, the least-square problem with Lagrange multiplier can be solved. To simplify calculations, the error function equation can be expressed as

$$\mathbf{G}^T \mathbf{W}_j \mathbf{G} \mathbf{a} = \mathbf{G}^T \mathbf{W}_j \mathbf{d} \quad (8)$$

The vector \mathbf{d} , \mathbf{a} , and matrix \mathbf{G} , \mathbf{W}_j are determined from \mathbf{D} matrix as follow.

$$\mathbf{d} = [\varepsilon_1 \cdots \varepsilon_n]^T, \quad \mathbf{a} = [a_1 \quad a_2]^T$$

$$\mathbf{G} = \begin{bmatrix} 1 & \cdots & 1 \\ x_1^m & \cdots & x_n^m \end{bmatrix}^T, \quad \mathbf{W}_j = \text{diag}(\omega_{ij}^{eff})$$

The prior information $\varepsilon(850) = a_1 + a_2 \times 850 = 0$ can be express as follows.

$$\mathbf{F} \mathbf{a} = 0 \quad (9)$$

$$\mathbf{F} = [1 \quad 850]$$

Using the Lagrange multiplier λ , the equations (8) and (9) can be express as follows.

$$\begin{bmatrix} \mathbf{G}^T \mathbf{W}_j \mathbf{G} & \mathbf{F}^T \\ \mathbf{F} & 0 \end{bmatrix} \begin{bmatrix} \mathbf{a} \\ \lambda \end{bmatrix} = \begin{bmatrix} \mathbf{G}^T \mathbf{W}_j \mathbf{d} \\ 0 \end{bmatrix} \quad (10)$$

$$\rightarrow \mathbf{A} \mathbf{p} = \mathbf{B}, \quad \mathbf{p} = \mathbf{A}^{-1} \mathbf{B}$$

From the calculated \mathbf{p} , the values a_{1j} and a_{2j} can be estimated.

- 5) Using the estimated strain distribution $\varepsilon_j(x) = a_{1j} + a_{2j}x$, calculate the residual value using equation (4). If the summation of v_{ij} does not become small enough, return to process 3), and repeat the weighted least-square method.

4.2 Results of Estimation

4.2.1 Estimated strain distribution and deflection

When the robust estimation method was carried out using distributed strain data from PPP-BOTDA system, the strain distribution and the deflection were able to be estimated. The results are shown in Fig.15 and Fig.16. The data, which was used for the estimation, was same as the data shown in Fig.12. Figure 15 shows the estimated strain distribution $\varepsilon_e(x) = a_{e1} + a_{e2}x$. From this estimated strain, the deflection can be estimated using the equation (2) in section 4.1, as shown in Fig.16. From the deflection, the estimation error, which is the difference between the estimated value and the measured value, is only +0.87 % at the distance $x=800$ m. The positive value of the estimation error means that the absolute value of the estimated deflection is larger than that of measured value. Therefore, it can be said that very reasonable the estimated deflection can be obtained by the proposed robust estimation method.

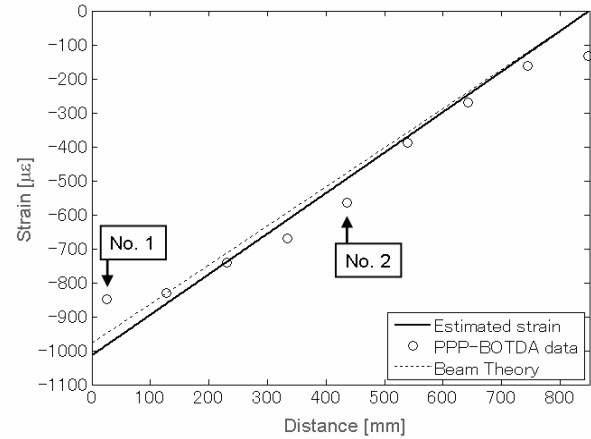


Fig. 15. Estimated strain distribution

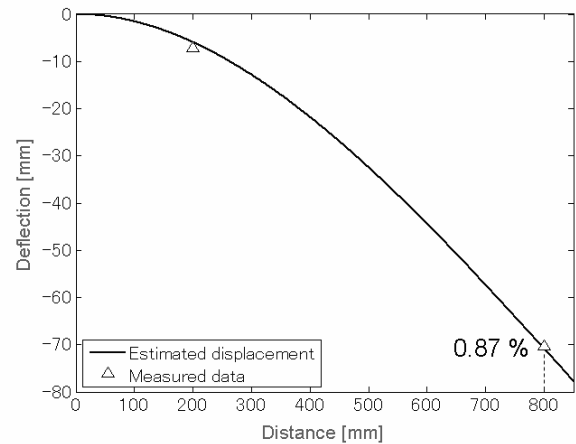


Fig. 16. Estimated displacement

4.2.2 Effects of robust estimation method

To verify the effectiveness of the robust estimation method, we compared estimated values between using the robust estimation method and using the least-square method. The least-square method was only the process 4) in section 4.1, and the weight values are 1 (no weight).

Firstly, we compared dispersions of estimation errors of deflection. In such inverse analysis, estimated values greatly depend on the strain data. Figure 17 is the plot of estimation errors of deflection, which are calculated by each estimation methods using ten different distributed strain data. From this result, estimation errors, which are calculated by the robust method, get generally lower than those by the least-square method. In addition, it can be said that the mean of estimation errors get near to zero by using the robust estimation method. This is because the data of the measurement point near the end of the beam specimen (measuring point No.1 in Fig.15), which has difference against theoretical strain distribution because of the influence of spatial resolution of 10 cm, has low weight in the robust estimation. From these results, it can be said that adjusted weights in the robust method work effectively in the estimation.

Secondly, the verification of the effectiveness against outliers was carried out. We made an outlier in the distributed strain data, which was used in the estimation in the section 4.2.1. The artificial outlier, $-50 \mu\epsilon$ or $-100 \mu\epsilon$, was added to one of the data points of distributed strain data (measuring point No.2 in Fig.15). And then, the robust estimation method was carried out using each distributed strain data. Figure 18 shows estimated strain distributions. From this figure, the plots of two estimated strain distributions were almost overlapped. Table 2 is the comparison of estimation errors of displacement between the value derived from the robust estimation method and that derived from the least-square method. Comparing the changes of estimation errors, there are little differences in the values derived from the robust estimation method. On the other hand, the values derived from the least-square method show larger fluctuations. Therefore, it can be said that the proposed method is robust against outliers of data.

From these verifications, it is shown that the robust estimation method is very suitable for the shape identification using distributed strain data from PPP-BOTDA system.

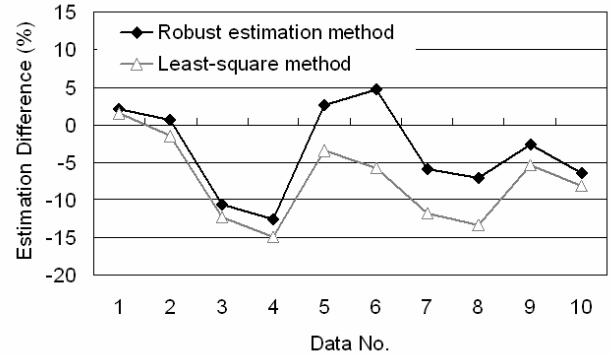


Fig. 17. Plot of the displacement estimation errors

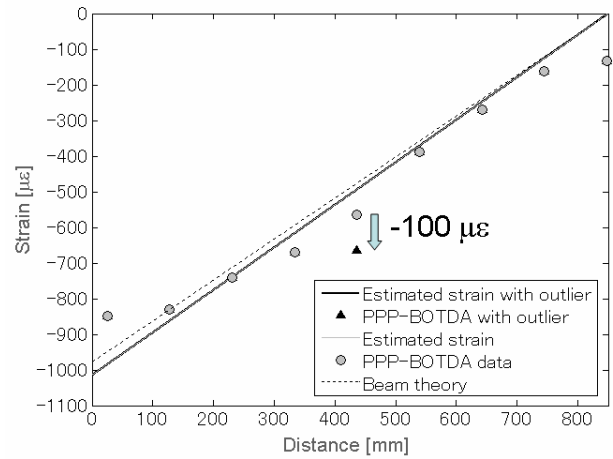


Fig. 18. Estimated strain with an artificial outlier

Table 2. Estimation error with outliers

Artificial Outlier	Robust estimation	least-square
$\pm 0 \mu\epsilon$ (raw data)	0.87 %	-1.48 %
$-50 \mu\epsilon$	0.93 % (+0.06)	-0.68 % (+0.80)
$-100 \mu\epsilon$	0.90 % (+0.03)	0.13 % (+1.61)

5 Conclusions

In this paper, we considered the shape identification method, which is suitable for the characteristic of the distributed strain data from PPP-BOTDA optical fiber sensing system. In the experiment, the distributed strain data were obtained by beam bending test using a composite beam specimen with an embedded optical fiber. It was shown that the strain distribution from PPP-BOTDA system was appropriate to the deflection of the

specimen. However, at the discontinuous point of the strain distribution along the fiber, the accurate value can not be obtained because of the influence of the spatial resolution of distributed data. Moreover, by verification of the measurement error distribution, it was shown that it was not strictly normal distribution and recognized some outliers and unpredictable shifts of distributions. From these results, we proposed the robust estimation method for shape identification algorithm, and verified the effectiveness of this method. By using this method, the estimation error of deflection was decreased, and the robustness against outliers of data was shown. As one of the future works, we will construct the robust shape identification method for more intricately deformation of composite structures.

Acknowledgement

One of the authors (M. Nishio) was supported through the 21st Century COE Program, “Mechanical Systems Innovation,” by the Ministry of Education, Culture, Sports, Science and Technology. In the fabrication of the specimen with VaRTM method, we received technical assistance from KADO Corporation. In addition, we received technical advices of the strain measurement using PPP-BOTDA system from Neubrex Co., Ltd, respectively.

References

- [1] A. Tessler, J.L. Spangler, “A Least-squares variational method for full-field reconstruction of elastic deformations in shear-deformable plates and shells,” *Computer method of applied mechanics and engineering*, 194, 327-339 (2005).
- [2] Philip B. Bogert, Eric Haugse, Ralph E. Gehrki, “Structural shape identification from experimental strains using a modal transformation technique,” *AIAA Paper*. 2003-1626.
- [3] Bao X., Brown A., Demercent M., Smith J., “Characterization of the Brillouin-loss spectrum of single-mode fibers by use of very short (<10 μ s) pulses,” *Optical Letters*, 24(8), 501-510 (1999).
- [4] K. Kishida, C.-H. Li, K. Nishiguchi, “Pulse pre-pump method for cm-order spatial resolution of BOTDA,” *Proceeding of the SPIE*, Volume 5855, 559-562 (2005).
- [5] A.E. Beaton, J.W. Tukey, “The fitting of power series, meaning polynomials, illustrated on band-spectroscopic data,” *Technometrics*, Vol.16, 147-192 (1974).